

Enhancing Resolution Using Iterative Back-Projection Technique for Image Sequences

Guo-Shiang Lin* and Min-Kuan Lai

Department of Computer Science and Information Engineering

Da-Yeh University

Changhua, Taiwan 51591, R.O.C.

khlin@mail.dyu.edu.tw

Received 5 October 2008; Revised 8 October 2008; Accepted 10 October 2008

Abstract. Resolution enhancement is a basic and important technology in image/video processing. The goal of resolution enhancement is to reconstruct high-resolution image frames from the corresponding low-resolution versions. In this paper, an adaptive resolution enhancement scheme based on iterative back-projection was proposed. According to sub-pixel interpolation, additional information composed of several low-resolution shifted images can be created. After giving initial estimates for each low-resolution shifted image, reconstructed high-resolution images are derived by using a modified iterative back-projection and then fused to be a high-resolution one. Finally, a post-processing is utilized to reduce the blocking artifacts within the reconstructed high-resolution images. According to performance comparison, the experimental results, in terms of PSNR and NQM, demonstrate that the proposed scheme is superior to these existing methods.

Keywords: resolution enhancement, image interpolation, iterative back projection

1 Introduction

High-resolution images are very useful in many applications, e.g., satellite imaging, medical imaging, video surveillance system, and automatic target recognition. The goal of resolution enhancement is based on the fact that a small amount of additional information among different views at the same scene can be utilized to construct a high-resolution image/video. It is expected that the resolution enhancement technique is very attractive. In fact, the resolution enhancement also called super-resolution is an ill-posed inverse problem [1-3], that is, there are many possible solutions for reconstructing a high-resolution (HR) image based on a set of observation images (i.e., low-resolution (LR) images) of the same scene. The accepted approach to deal with the problem is to constrain the solution space according to prior knowledge on the form of the solution.

According to [4], resolution enhancement techniques can be generally classified into three categories: single-image, multi-frame, and image sequence (video). In each single-image approach also called image interpolation, each image frame is individually processed, i.e., only the spatial-domain information within each image frame is exploited to improve the reconstructed version [5-9]. In [8], some interpolation algorithms such as zero-order interpolation and bilinear interpolation are often adopted to achieve image enlargement and local image zooming. However, image artifacts like blurring or zigzag on edge may occur as simple interpolation strategies are utilized. This means that one important issue of reconstructing a HR image is how to deal with image edges to lessen these artifacts in an adequate way. In order to reduce the effect of image artifacts, some edge preserving methods have been proposed [6, 7]. In [7], interpolated values along different directions are computed by using the corresponding weights depending on the variation in the directions. Besides, to recover the high frequency components of a HR image, some image synthesis methods [10, 11] were proposed. For instance, authors [10] proposed a resolution synthesis method in which a pre-processing step is to divide an image into many patches and classify these patches into several classes. To classify the image patches, some training images are exploited to devise a set of filters. For the classes containing edges, the interpolation method with trained parameters obtained by optimizing the training samples is utilized. For the classes without edges, a simple method, e.g., bilinear interpolation, is utilized.

In the multi-frame resolution enhancement methods, several image frames of the same scene with only camera shift are exploited to interpolate a HR image frame at the same scene. In [12], the multi-frame resolution enhancement problem was first addressed and a frequency domain approach was proposed. Although the fre-

* Correspondence author

quency-domain approaches are simple and computationally cheap, they are sensitive to model errors. In [13], Kim et al. proposed a method to reconstruct a HR image from a sequence of LR, under-sampled, noisy, and blurred image frames. For image sequence resolution enhancement also called dynamic super-resolution [4],[5],[14],[15],[16] both the spatial and temporal information available in a LR image sequence can be used to restore the HR versions. For example, Chen et al. [14] proposed a multi-frame resolution enhancement method in which smooth pixels are first interpolated and then edge pixels are further processed. In [4], a method where an initial estimate of each HR image frame is derived by using cubic interpolation and then a refinement is applied to reconstruct each final HR version was proposed. Basically, only spatial information is taken into account in the above two methods.

Until now, most researchers focus on single-image resolution enhancement [1],[6],[7],[9]. Only few researchers have addressed the issue of image sequence resolution enhancement. Therefore, we aim at developing a resolution enhancement scheme for image sequences based on iterative back projection (IBP) technique in this paper. After obtaining a small amount of additional information with different views at the same scene, a modified IBP algorithm in the proposed resolution enhancement scheme is then developed to simultaneously derive the image details but also achieve the edge preserving of each HR image.

The remainder of this paper is organized as follows. Section II introduces the proposed resolution enhancement scheme. In Section III, we detail then experimental results. Then, in Section IV, we present our conclusions.

2 Adaptive resolution enhancement scheme

2.1 Problem formulation

Before describing the proposed resolution enhancement scheme, we first formulate the problem of resolution enhancement. In theory, the generation process of a LR image can be modeled as a HR image suffering from a combination of the blurring and the down-sampling operations. The blurring operation may result from an optical system, relative motion between the imaging system and the original scene, and the point spread function (PSF) of the LR sensor. By simplifying the blurring, motion, and sub-sampling with the scaling factor z into a single filter H for the entire image, the generation process of a LR image G_i from a HR image F can then be formulated as follows:

$$G_i = H_i F + V_i, \quad i = 1, \dots, N^L, \quad (1)$$

where F and G_i are the HR image and the i -th observed LR ones, respectively; V_i is the additive noise existing in any imaging system for G_i ; N^L represents the number of LR images. According to Eq. (1), the LR image is the decimated and blurry outcome with additive noises. It is expected that the larger the scaling factor and noises are, the quality of a reconstructed HR image has. Without loss of generality, we assume that F and G_i are square images and their sizes are $N^W \times N^W$ and $zN^W \times zN^W$, respectively.

According to [1], [3], [4], and [9], the PSF is usually modeled as a space-invariant averaging filtering in the spatial domain, and the down-sampling and blurring operations are usually time-invariant. In addition, we pay attention to a common case that the motion between frames is pure translation. As a matter of fact, this assumption is very suitable in more practical applications such as satellite image enhancement. Therefore, a simplified model composed of (a) spatial/temporal-invariant blurring and mean-value decimator, and (b) translational motion is adopted in this paper. This means that each LR frame is considered as a shifted, uniformly down-sampled, and blurred version of a HR image under the conditions: $H = H_i$ and $V = V_i$. Thus, Eq. (1) can be rewritten as

$$G_i = HF + V, \quad i = 1, \dots, N^L. \quad (2)$$

As shown in Eq. (2), some adjacent LR images are related to one HR image. In this paper, we only consider the simplest case: $N^L = 1$.

2.2 Review of iterative back projection

Iterative back-projection [1] (IBP) is an efficient algorithm to acquire the HR image by minimizing the norm of the reconstruction error. Given an estimate of the reconstructed HR image and a model of the imaging process, a

set of simulated LR images can then be generated. Each simulated LR image is compared with the actual version and then the error can be used for correcting the estimated HR image. In fact, it is difficult to restore a HR image in a one-shot manner. Hence, an iterative procedure is needed. This simulate/correct process is iterated until some stopping condition is achieved. Generally, the minimization of some error criterion between the simulated and observed LR images is adopted as the stopping condition.

According to the above mention, the advantage of IBP is that it is simple and easy to integrate with the spatial-domain observation model and priori information. Its disadvantage is that the edges in the reconstructed HR image are often blurred and some artifacts, e.g., chessboard effect, may be incurred. Thus, a modified IBP is proposed to not only reconstruct the HR image but also achieve edge preserving in this paper.

2.3 Proposed resolution enhancement scheme

In [4] and [14], each pixel value of the reconstructed HR image frame is interpolated only according to the neighboring pixels in the LR image. In this paper, the additional information is a set of several shifted LR versions gathered from the spatial domain. Each LR image and its shifted versions are individually used to estimate the immediate HR ones by using a modified IBP. Then these immediate HR images are fused to derive the final HR version. The schematic diagram of the proposed scheme is shown in Fig. 1.

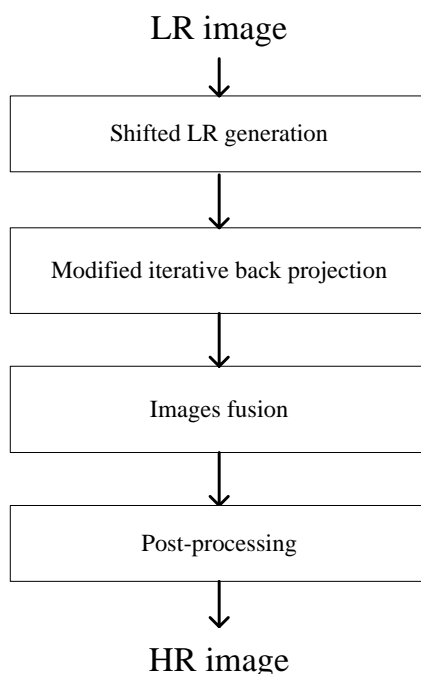


Fig. 1. The schematic diagram of proposed resolution enhancement scheme

Before introducing the proposed scheme in detail, we first define the operating unit as a block of size $z \times z$. Then a HR image is partitioned into many non-overlapping and equal-sized operating units, in which each operating unit corresponds to a pixel in the LR (decimated) image. Fig. 2 illustrates an operating unit shown as the dashed box as z is 2. As we can see in Fig. 2, an operating unit contains four pixels and each pixel results from its corresponding shifted LR image frame.

Shifted LR generation. In order to derive extra information, we compute the sub-pixel values in each LR image by using the bilinear interpolation to obtain some shifted LR images. Here the bilinear interpolation is used to create the initial HR solution based on the input LR image. In fact, other interpolation methods can replace the bilinear interpolation for generating an initial HR solution. Fig. 2 illustrates the relation between the shifted LR images and the corresponding HR image as z is 2. These shifted LR images can be expressed as $\hat{g}_{i,j}$ ($0 \leq i, j < z$). In Fig. 2, $\hat{g}_{i,j}(m,n)$ indicates the shifted version of $\hat{g}_{0,0}(m,n)$ with i ($1/z$)-pixel down and j ($1/z$)-pixel to the right, where (m,n) represents the coordinate in the LR image.

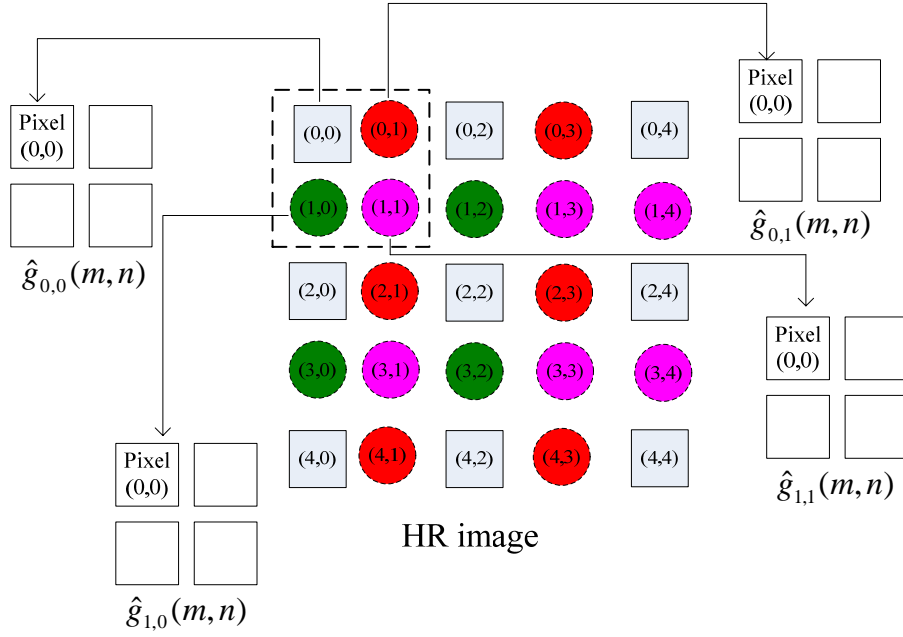


Fig. 2. An illustration of the relation between the shifted LR images and corresponding HR image in the spatial domain

Denote $\hat{f}_{i,j}$ as the corresponding LR image of $\hat{g}_{i,j}$. After each shifted LR image is obtained, each corresponding initial HR solution can be calculated. Based on the relation among the LR images ($\hat{g}_{0,0}(m,n)$, $\hat{g}_{0,1}(m,n)$, $\hat{g}_{1,0}(m,n)$, and $\hat{g}_{1,1}(m,n)$) in the spatial domain, we can acquire the initial solutions of the HR image, $\hat{f}_{0,0}^{(0)}(k,l)$, $\hat{f}_{0,1}^{(0)}(k,l)$, $\hat{f}_{1,0}^{(0)}(k,l)$, and $\hat{f}_{1,1}^{(0)}(k,l)$, respectively, where (k,l) denotes the coordinate in the HR image. Note that $\hat{f}_{i,j}^{(0)}(k,l)$ indicates the shifted version of $\hat{f}_{0,0}^{(0)}(k,l)$ with i pixel down and j pixel to the right, where (k,l) denotes the coordinate in the HR image.

Modified iterative back-projection. After getting shifted LR images and the corresponding initial HR images, each reconstructed HR image can be derived individually by using a modified IBP. Figure 3 illustrates the modified IBP and we elaborate the modified IBP in the following. As stated in Section 2.2, the disadvantage of IBP is to blur the discontinuous areas of the reconstructed version. The reason is that an insufficient result may be achieved due to the only object of minimizing the reconstruction error in IBP. To reduce the smoothness and artifacts resulting from the inadequate result, sophisticatedly updating the guess of the HR image is necessary.

The differences between the proposed IBP and the traditional version are error compensation for updating the HR image and the measurement between the input LR image and its simulated version. To achieve edge preserving, the error compensation is performed according to the local property, i.e., edge information. In addition, it is important to reconstruct a HR image with high visual quality for human eyes. To improve the visual quality, a measurement NQM (noise quality metric) proposed in [17] (claimed to be a better measure than PSNR for additive noises) is adopted to evaluate the similarity of the input LR image and its simulated version based on human visual system. It is expected that a reconstructed HR image with a high visual quality can be derived. Note that the iterative algorithm will stop if the difference of visual quality (i.e., NQM) of the reconstructed HR image between two adjacent iterations is less than a predefined threshold or the number of iterations is higher than a given threshold.

Without loss of generality, we first use $\hat{g}_{i,j}(m,n)$ and $\hat{f}_{i,j}^{(0)}(k,l)$ to explain the modified IBP in detail. According to the assumption mentioned in Section 2.1, the simulated LR image can be calculated as

$$\tilde{g}_{i,j}^{(p)}(m,n) = \left[\frac{1}{z^2} \sum_{k=zm}^{zm+z-1} \sum_{l=zn}^{zn+z-1} \hat{f}_{i,j}^{(p)}(k,l) \right], \quad 0 \leq i,j < z, \quad (3)$$

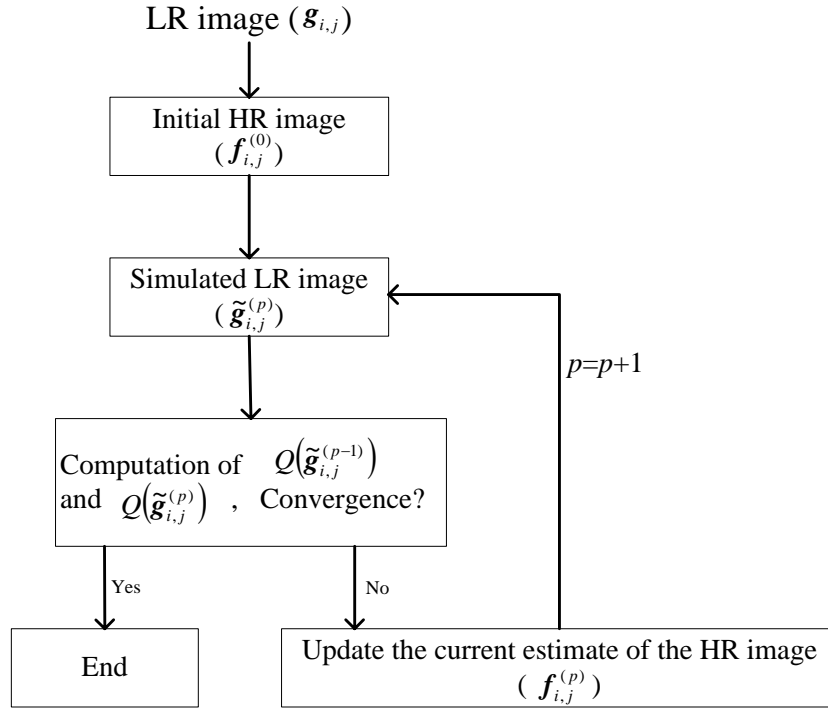


Fig. 3. The flowchart of modified IBP

where p denotes the iteration number ($p \geq 0$), $\tilde{g}_{i,j}(m,n)$ is the (m,n) pixel value of the simulated LR image in the p -th iteration, and $[\cdot]$ denotes the rounding operator. Then the visual quality of the simulated LR image in the p -th iteration is expressed as $Q(\tilde{g}_{i,j}^{(p)})$, where $Q(\cdot)$ denotes the NQM metric and $\tilde{g}_{i,j}^{(p)} = \{\tilde{g}_{i,j}^{(p)}(m,n), 0 \leq m, n < N^W\}$. As shown in Fig. 3, whether the current guess of the HR image in the p -th iteration replaces the previous one is determined according to the difference of the visual quality of the LR input image and the simulated LR version between two adjacent iterations. The rule of updating the current estimate is described as follows:

$$\hat{f}_{i,j}^{(p+1)} = \hat{f}_{i,j}^{(p)} \cdot U(Q(\tilde{g}_{i,j}^{(p)}) - Q(\tilde{g}_{i,j}^{(p-1)})) + \hat{f}_{i,j}^{(p-1)} \cdot (1 - U(Q(\tilde{g}_{i,j}^{(p)}) - Q(\tilde{g}_{i,j}^{(p-1)}))), \quad (4)$$

where $U(\cdot)$ denotes the unit step function with output +1 or 0. As shown in Eq. (4), the $(p+1)$ -th HR image is updated by the (p) -th version if $Q(\tilde{g}_{i,j}^{(p)})$ is more than $Q(\tilde{g}_{i,j}^{(p-1)})$.

To update the current estimate of the HR image, the difference between the LR input image and the simulated LR version is first defined as follows:

$$\hat{r}_{i,j}^{(p)}(m,n) = \hat{g}_{i,j}(m,n) - \tilde{g}_{i,j}^{(p)}(m,n), \quad 0 \leq i, j < z, \quad (5)$$

where $\hat{r}_{i,j}^{(p)}(m,n)$ ($0 \leq i, j < z$) denotes the error of pixel values between the LR input image and the simulated LR version at the (m,n) coordinate in the p -th iteration. To take the observation noise into account, a data consistency constraint can be utilized and expressed as

$$|\hat{r}_{i,j}^{(p)}(m,n)| < \eta, \quad (6)$$

where η is a pre-defined threshold and may be determined according to the noise statistics. It is expected that the smaller the $|\hat{r}_{i,j}^{(p)}(m,n)|$ is, the better the approximation of each pixel in the operation unit is.

As we know, compared with smooth areas, high-contrast edges are more sensitive by human eyes. After generating the initial solution by using the bilinear interpolation, the discontinuities are often smoothed to result in a

blurry image frame. To deal with this problem, an adaptive error compensation algorithm for updating the HR image is proposed here to reduce the oversmoothing effect. According to [4], it is assumed that the edges in the LR image frame also generally exist in the corresponding HR image frame. That means that the edge information can be extracted from the LR image and useful to perform adaptive error compensation in modified IBP.

Basically, each pixel value in the reconstructed HR image can be formulated as follows:

$$\hat{f}_{i,j}^{(p+1)}(k,l) = \hat{f}_{i,j}^{(p)}(k,l) + \hat{w}_{i,j}(k,l) \cdot \text{sgn}(\hat{r}_{i,j}^{(p)}(m,n)) \cdot \left(\left| \hat{r}_{i,j}^{(p)}(m,n) \right| - \eta \right) \cdot U \left(\left| \hat{r}_{i,j}^{(p)}(m,n) \right| - \eta \right), \quad (7)$$

where $\hat{w}_{i,j}(k,l)$ is the weight and $\text{sgn}(\cdot)$ is the sign function with output +1 or -1. As we can see, $U \left(\left| \hat{r}_{i,j}^{(p)}(m,n) \right| - \eta \right)$ indicates whether the error compensation is adopted or not. This means that the error compensation happens only as $\left| \hat{r}_{i,j}^{(p)}(m,n) \right|$ is more than the pre-defined threshold η . The scale, $\text{sgn}(\hat{r}_{i,j}^{(p)}(m,n)) \cdot \left(\left| \hat{r}_{i,j}^{(p)}(m,n) \right| - \eta \right)$, represents the desired compensated error.

To consider the spatial-domain information within each shifted LR image frame for pixel classification, Canny edge detector [8] is adopted to generate an edge map here. In the edge map, we classify the LR image into two classes: homogeneous and edge areas. Then the error compensation in the back-projection is adaptive according to the edge map and local properties in each operating block. The error compensation is described in the following.

(a) Homogeneous area

As mentioned in Section 2.1, each LR frame is considered as a shifted, uniformly down-sampled, and blurred version of a HR image. Then the corresponding weight of each homogeneous pixel for error compensation is defined as follows:

$$\hat{w}_{i,j}(k,l) = \frac{1}{z^2}. \quad (8)$$

As shown in Eq. (8), the errors are equally distributed into each pixel in the operating unit.

(b) Edge area

Since the equal weight in Eq. (8) makes edges blurry, the basic idea for reducing the smoothing effect is that the compensated errors for updating the HR image are distributed according to the content of the operating unit. Here we take the direction of gradient of pixel values and the sign of the compensated error into account to adaptively distribute the error to pixels in the operating unit. In order to perform this idea, the weight of each pixel in the edge area is determined in the following cases:

Case 1: $r_i > \eta$

According to Eq. (7), the pixel values of the reconstructed HR image should be increased in this case. To achieve edge preserving and reduce blurring effect, the goal in this case is that the higher the pixel value is, the larger the weight is. Then the weight in Case 1 is defined as

$$\hat{w}_{i,j}(k,l) = \frac{\hat{f}_{i,j}^{(p)}(k+i,l+j)}{\sum_{i=0}^{z-1} \sum_{j=0}^{z-1} \hat{f}_{i,j}^{(p)}(k+i,l+j)}, \quad 0 \leq i,j < z. \quad (9)$$

As we can see in Eq. (9), the weight of the pixel with high pixel value is larger than that of the pixel with low pixel value. It is expected that the edge in the operating unit can be maintained.

Case 2: $r_i < -\eta$

In this case, the pixel values of the reconstructed HR image should be reduced. Compared with Case 1, the rule is that the higher the pixel value is, the smaller the weight is. Then the weight in Case 2 is defined as

$$\hat{w}_{i,j}(k,l) = \frac{\hat{S}_{i,j}^{(p)}(k+z-1-i',l+z-1-j')}{\sum_{i=0}^{z-1} \sum_{j=0}^{z-1} \hat{S}_{i,j}^{(p)}(k+i,l+j)} \cdot \delta(\hat{f}_{i,j}^{(p)}(k+i,l+j) - \hat{S}_{i,j}^{(p)}(k+i',l+j')), \quad (10)$$

where $\hat{S}_{i,j}^{(p)}(k+i',l+j')$ denote the sorted result of $\hat{f}_{i,j}^{(p)}(k+i,l+j)$ according to the decreasing order, $\delta(\cdot)$ is an impulse function, and (i',j') represents the index after sorting ($0 \leq i',j' < z$). In the same manner, maintaining the edge in the operating unit can be achieved.

Image fusion. After updating current solution of each HR image, a combined $\hat{\mathbf{F}}$ based on the z HR images created in the spatial domain can be calculated as follows:

$$\hat{\mathbf{F}} = \left\{ \hat{f}(k,l) \mid \hat{f}(k,l) = \frac{1}{z^2} \sum_{i,j=0}^{z-1} \hat{f}_{i,j}^{(p)}(k,l), 0 \leq k,l < zN^w \right\}. \quad (11)$$

Post-processing. In fact, the blocking effect resulting from the error compensation in each operating block may be visible on the edge part of the reconstructed HR image. To reduce the impact of blocking effect on the edge part of the reconstructed HR image, a post-processing is developed here. According to the edge map, only the boundary pixels of the neighboring operating units next the edges are processed with their pixel values being modified as the corresponding output values of Gaussian low-pass filter centered at the pixels to be processed.

3 Experimental results

To evaluate the performance of our proposed algorithm and compare it with some existing methods, Bilinear interpolation (BI), Cubic interpolation (CI), and [18], we selected 20 images, each composed of 512×512 pixels, and several image sequences, 100 frames and each frame composed of 352×288 pixels, as subjects. We conducted several experiments to evaluate the performances of the proposed scheme. In addition to the traditional PSNR, NQM [17] was also adopted to measure the picture quality based on an HVS model. In this paper, two different scaling factors ($z = 2$ and 4) along the horizontal and vertical directions, and the mean-value decimator are used to create LR images. The parameter η in Eq. (6) and the number of iterations are set to be 2 and 5 in the following experiments, respectively.

3.1 Performance evaluation

First, we use 20 still images to evaluate the proposed scheme. Fig. 4 illustrate some reconstructed HR images under the case: $z=2$. As shown in Fig. 4, these reconstructed HR images have good visual quality. In addition, we analyze the impact of the number of iterations on the image quality of the restored HR image.

To analyze the effect of the error compensation for updating the HR image and quality measurement, we make a comparison with the traditional IBP. As shown in Figs. 5 and 6, PSNR and NQM of each test image for our proposed scheme are higher than those for IBP under $z=2$. The average PSNR and NQM of our proposed scheme are 29.38 dB and 34.81 dB, respectively. In addition, for PSNR, the minimum and maximum values of improvement are 0.76 dB and 2.94 dB, respectively. Similarly, the minimum and maximum values of improvement of NQM are 5.98 dB and 10.3 dB, respectively. These results show the performance of our proposed scheme is better than that of IBP in terms of PSNR and NQM. These results also demonstrate that the error compensation for updating the HR image and quality measurement (i.e., NQM) of our proposed scheme did advance the visual quality.

Table 1 shows that average PSNRs and NQMs of 20 test images under different scaling factors ($z=2$ and 4). As we can see in Table 1, the average PSNR and NQM of the proposed scheme are high as z is small. The results match our analysis in Section 2.1.



Fig. 4. Reconstructed HR images: (a) Lean, (b) Elaine, and (c) Pepper

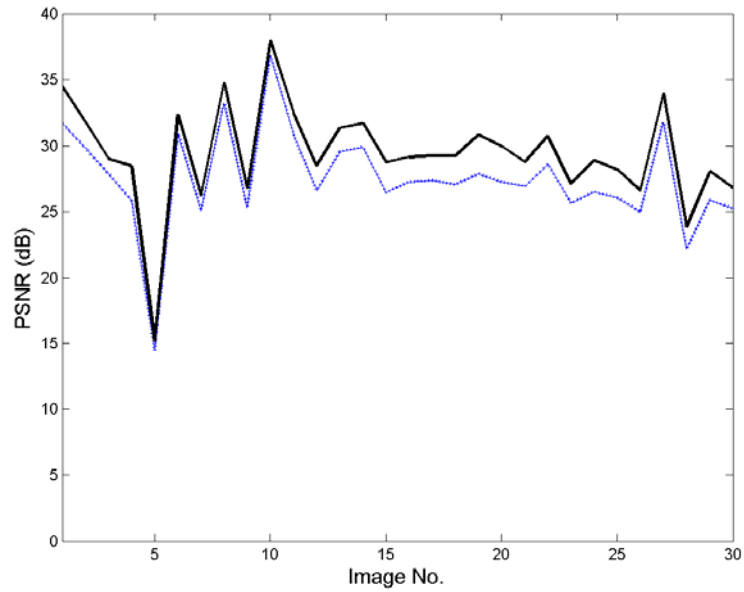


Fig. 5. PSNRs of Proposed scheme and IBP: Proposed: solid line; IBP: dotted line

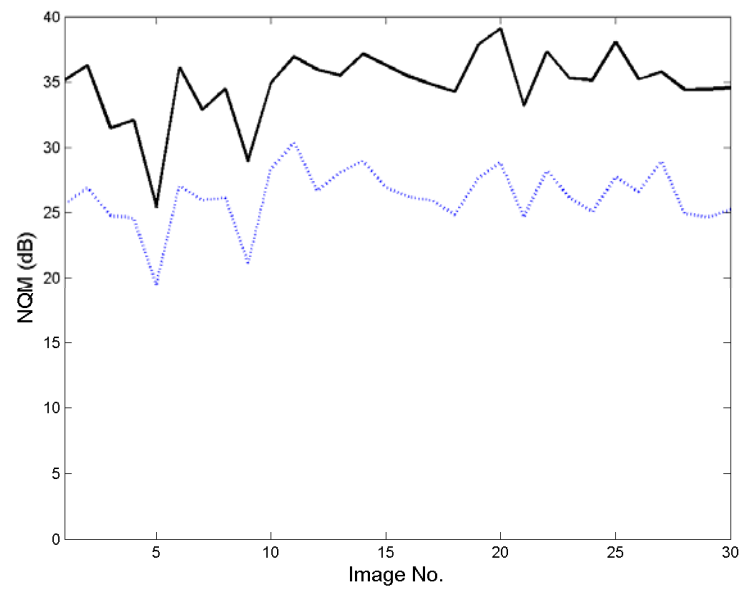


Fig. 6. NQMs of Proposed scheme and IBP: Proposed: solid line; IBP: dotted line

3.2 Comparison with existing methods

Some existing methods, BI, CI, and [18], are used to make comparisons and then the experimental results are also shown in Tables 1 and 2. For 20 test images, the average PSNR and NQM of the proposed scheme are higher than those of the others under different the scaling factors of down-sampling. Since the performance of CI is the best among the existing methods, the phenomenon that compared with CI, there are improvements of 2.76 dB and 10.23 dB in PSNR and NQM for the proposed scheme under $z=2$. For $z=4$, the PSNR and NQM of the proposed scheme are still higher (3.42 dB and 10.73 dB) than those of CI, respectively. These experimental results demonstrate the performance of our proposed scheme is better than those of the others in terms of PSNR and NQM.

Table 1. The average PSNRs and NQMs of 20 test images compared with BI, CI, and [18]

	BI		CI		[18]		Proposed	
	PSNR (dB)	NQM (dB)						
$z=2$	26.69	24.27	27.15	24.33	26.40	23.79	29.91	34.56
$z=4$	21.24	14.43	21.37	14.12	21.24	14.23	24.79	24.85

Table 2. The average PSNRs and NQMs compared with BI, CI, and [18] ($z=2$)

	BI		CI		[18]		Proposed	
	PSNR (dB)	NQM (dB)						
Stefan	23.28	22.95	23.79	23.50	23.21	23.26	25.45	29.69
Toy Train	19.53	19.97	19.91	20.02	19.46	19.30	21.08	28.12
Table Tennis	26.11	24.63	25.67	24.72	25.29	24.26	28.39	34.40

Here we also use three image sequences to make performance comparison. The PSNR of each frame is shown in Fig. 7 as the sequence “Table Tennis” is tested and $z=2$. As we can see in Fig. 7, the PSNR of each frame in the proposed scheme is higher than those in the existing methods. Compared with CI, the maximum and minimum values of PSNR improvement for the proposed scheme are 3.01 and 2.33 dB, respectively. In addition, as the sequence “Table Tennis” is tested, the NQM of each frame is shown in Fig. 8 and the average of NQMs is 34.39 dB. At the same manner, compared with CI, the maximum and minimum values of NQM improvement for the proposed scheme are 10.75 and 7.81 dB, respectively. As mentioned above, the experimental results demonstrate that the performance of our proposed scheme is better than those of the existing methods according to the viewpoint of visual quality.

The average PSNRs and NQMs of the proposed scheme and the existing methods for 3 test sequences are listed in Table 2 under $z=2$. As observed in Table 2, the average PSNR and NQM of the proposed scheme are 24.97 dB and 30.74 dB, respectively. In addition, the average PSNRs and NQMs of the proposed scheme are higher than those of the others. Compared with CI, the PSNR and NQM improvement for the proposed scheme are 1.85 and 7.99 dB, respectively. According to the above results, the proposed scheme is superior to the existing methods (BI, CI, and [18]) in terms of PSNR and NQM.

4 Conclusion

In this paper, an adaptive resolution enhancement scheme based on iterative back-projection was proposed. According to sub-pixel interpolation, additional information composed of several low-resolution shifted images can be obtained. After deriving initial estimates for each low-resolution shifted image, a modified iterative back-projection is exploited to reconstruct the information lost from the HR image but also achieve the edge preserving. Finally, a post-processing is utilized to reduce the blocking artifacts within the reconstructed high-resolution images.

For performance evaluation, 20 images and three image sequences are tested. For 20 images, there are improvements of 2.76 dB and 10.23 dB in PSNR and NQM for the proposed scheme as compared with CI. Similarly, the increments of PSNR and NQM for the proposed scheme are respectively 1.85 dB and 7.99 dB for three test sequences. According to the experimental results, in terms of PSNR and NQM, the reconstructed results by the proposed scheme are better than those of three existing methods for performance comparison.

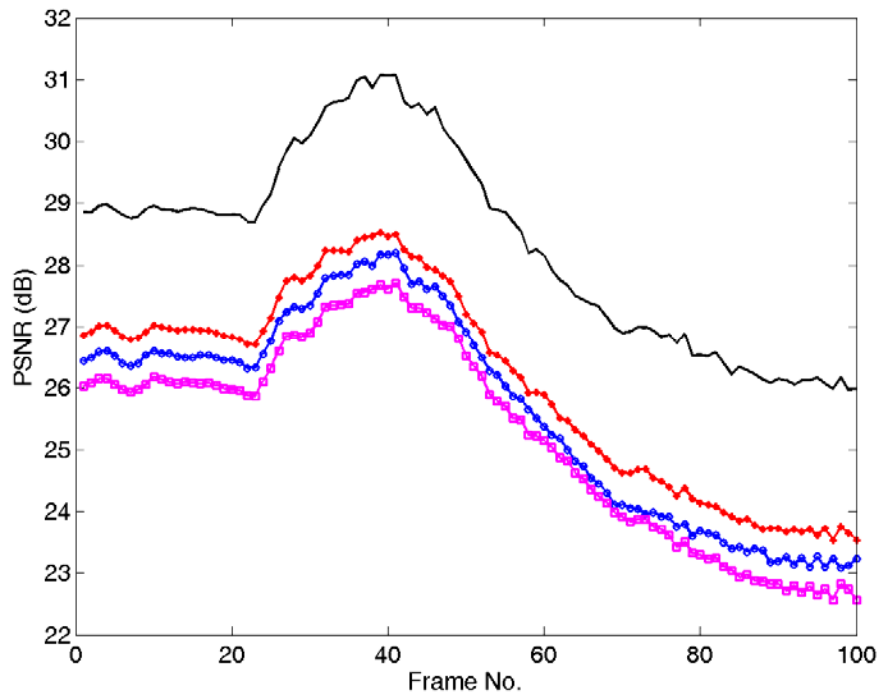


Fig. 7. The PSNR of each frame for Table Tennis: Proposed : solid line; “O”, “*”, and “■” represent CI, BI, and [18], respectively

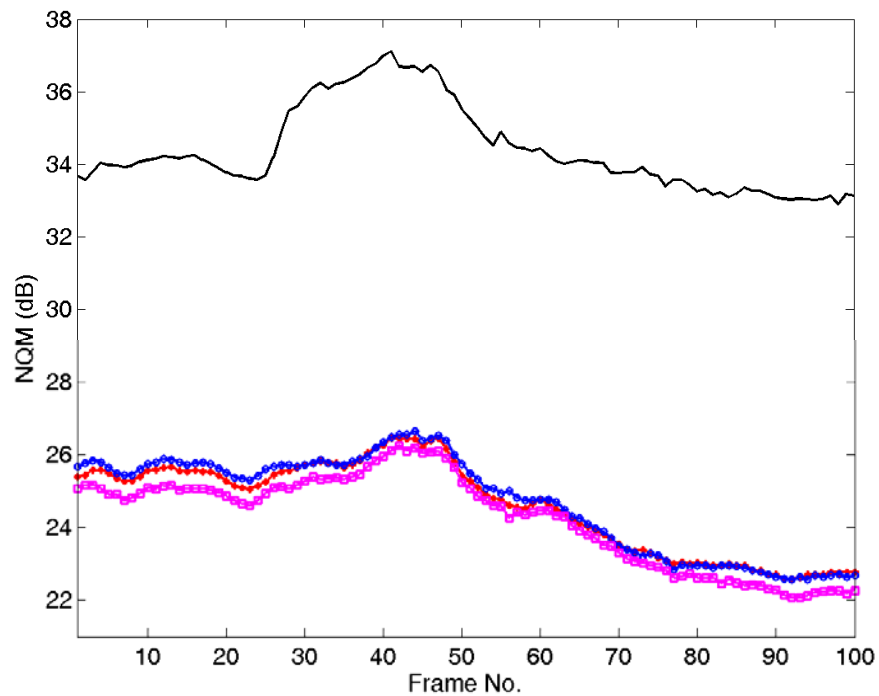


Fig. 8. The NQM of each frame for Table Tennis: Proposed : solid line; “O”, “*”, “◆”, and “■” denote CI, BI, and [18], respectively

References

- [1] S. C. Park, M. K. Park, and M. G. Kang, "Super-resolution image reconstruction_ a technical overview," *IEEE Signal Processing Magazine*, Vol. 20, pp.21-36, 2003.
- [2] M. Elad and Y. Hel-Or, "A fast super-resolution reconstruction algorithm for pure translational motion and common space invariant blur," *IEEE Transactions on Image Processing*, Vol. 10, pp.1187-1193, 2001.
- [3] F. M. Candocia and J. C. principle, "Super-resolution of images based on local correlation," *IEEE Transactions on Neural Network*, Vol. 10, pp.372-380, 1999.
- [4] C.-S. Chuah, and J.-J. Leou, "An adaptive image interpolation algorithm for image/video processing," *Pattern Recognition*, Vol. 34, pp.2383-2393, 2001.
- [5] H.-H. Wu, M.-H. Sheu, and T.-Y. Yang, "Directional Interpolation for Field-Sequential Stereoscopic Video," *Proc. IEEE International Symposium on Circuits and Systems*, pp.2879-2882, 2005.
- [6] X. Li and M. T. Orchard, "New edge-directed interpolation," *IEEE Transactions on Image Processing*, Vol. 10, pp.1521-1527, 2001.
- [7] S.D. Bayraker, R.M. Mersereau, "A new method for directional image interpolation," *Proc. IEEE International Conf. on Acoustics, Speech, and Signal Processing*, pp.2383-2386, 1995.
- [8] M. Sonka, V. Hlavac, and R. Boyle, *Image processing, analysis, and machine Vision*, Thomson, 2008.
- [9] L. Zhang and X. Wu, "An edge-guided image interpolation algorithm via directional filtering and data fusion," *IEEE Transactions on Image Process.*, Vol. 15, No. 8, pp.2226-2238, 2006.
- [10] C. B. Atkins, C. A. Bouman, and J. P. Allebach, "Tree based resolution synthesis," *Proc. Conf. on Image Processing, Image Quality, Image Capture Systems*, pp.405-410, 1999.
- [11] W. T. Freeman, T. R. Jones, and E. C. Pasztor, "Example-based super-resolution," *IEEE Computer Graphics and Applications*, Vol. 22, pp.56-65, 2002.
- [12] N. K. Bose, H. C. Kim, and H. M. Valenzuela, "Recursive implementation of total least squares algorithm for image reconstruction from noisy undersampled multiframes," *Proc. IEEE Int. Conf. Acoustics, Speech, and Signal Processing*, pp. 269-272, 1993.
- [13] S. P. Kim and W.Y. Su, "Recursive high-resolution reconstruction of blurred multiframe images," *IEEE Transactions on Image Process.*, Vol. 2, pp.534-539, 1993.
- [14] M.-J. Chen, C.-H. Huang, and W.-L. Lee, "A fast edge-oriented algorithm for image interpolation," *Image and Vision Computing*, Vol. 23, pp.791-798, 2005.
- [15] W. Y. Su and S. P. Kim, "High-resolution restoration of dynamic image sequences," *Int. J. Imaging Systems Technol.*, Vol. 5, pp. 330-339, 1994.
- [16] T. Madhusudhan and A. R. Pais, "Generation of super-resolution video from low resolution video sequences: a novel approach," *Proc. Int. Conf. Computational Intelligence and Multimedia Applications*, pp.255-232, 2007.
- [17] N. Damera-Venkata, T.-D. Kite, W.-S. Geisler, B.-L. Evans, and A.- C. Bovik, "Image quality assessment based on a degradation model," *IEEE Transactions on Image Processing*, Vol. 9, pp.636-650, 2000.
- [18] L. Rodrigues, D. Leandro Borges, and L. Marcos Goncalves, "A locally adaptive edge-preserving algorithm for image interpolation," *Proc. IEEE Proceedings XV Brazilian Symposium on Computer Graphics and Image Processing*, pp.300-305, 2002.